Sustainable Energy & Fuels

PAPER

View Article Online
View Journal | View Issue

Check for updates

Cite this: *Sustainable Energy Fuels*, 2022, **6**, 2718

Impact of lifetime on the levelized cost of electricity from perovskite single junction and tandem solar cells†

Ramez Hosseinian Ahangharnejhad,[a] Adam B. Phillips,[a] Zhaoning Song,[a] Ilke Celik,[b] Kiran Ghimire,[a] Prakash Koirala,[a] Randy J. Ellingson,[a] Robert W. Collins,[a] Nikolas J. Podraza,[a] Yanfa Yan[a] and Michael J. Heben*[a]

Received 7th January 2022
Accepted 25th April 2022

DOI: 10.1039/d2se00029f

rsc.li/sustainable-energy

With high efficiency and fast processing, metal halide perovskite (PK) solar cells promise a new paradigm for low-cost solar power. In addition to single junction device performance that is near the internal Shockley–Queisser limit, new tandem configurations promise even higher efficiencies. Efforts to commercialize PK-based modules are hindered by several factors including questions of cost and performance in the field. Long lifetimes are needed to achieve a low levelized cost of electricity (LCOE) and establish bankability. To understand the impact of device lifetime on LCOE we compared bottom-up cost and energy yield analyses for single-junction and tandem solar modules based on optical modeling of the device stacks, the device physics, and real-world advanced irradiance and temperature variation data. The degradation rate was taken to be a variable to examine the impact of stability on the LCOE. We show that both device and field lifetimes are critical to achieve a low LCOE for a solar power station. Additionally, for all PK device lifetimes, tandems constructed with higher-cost tandem partners will be economically disadvantaged in the market place.

Introduction

As single junction (SJ) photoconversion efficiencies for thin-film photovoltaic (PV) devices approach the internal Shockley–Queisser (iSQ) thermodynamic limit for the particular device constructions, efficiency gains are more difficult to achieve. Consequently, there is a growing interest in tandem devices. Of particular interest are tandem solar cells based on metal halide perovskites (PKs). PKs offer a wide variety of low temperature processing routes and bandgaps that can be readily varied between ~1.25 and ~3.1 eV.[1] Large bandgap PK materials can be used as top cells that can be paired with lower bandgap bottom cells fabricated with Si,[2–4] $Cu(In_xGa_{1-x})Se_2$ (CIGS),[5–11] and small-gap PKs.[12–18] Current AM1.5G record power conversion efficiencies (PCEs) are 29.8% (ref. 19) and 27.7% (ref. 20) for two- and four-terminal (2T and 4T) PK/Si devices, respectively. For all-thin-film configurations, efficiencies of 24.2% (ref. 19) and 25.9% (ref. 11) have been achieved for PK/CIGS devices in 2T and 4T devices, respectively, while 26.4% (ref. 12) and 25% (ref. 13) have been shown for 2T and 4T PK/PK constructions. There are now several examples of tandems that have efficiencies that exceed the record efficiency of both individual subcells,[21] and thermodynamically-limited 1 sun efficiencies up to 34% can be expected in the future (*vide infra*). Decisions regarding large scale manufacturing will depend not only on the cost of materials and equipment acquisition and operation, but also on the expected performance and longevity of PK-based modules in the field.

While PCE is a good metric for improving device performance in the lab, the decision to pursue a proposed PV system is based on the expected levelized cost of electricity (LCOE) for the installed system. LCOE (eqn (1)) is the net present value of all costs for building and operating an electricity generating system over a given deployment time in the field, divided by the energy yield (EY) expected during that time. For a consumer, LCOE can be used to compare the costs of electricity production across a variety of options.[22,23]

$$\mathrm{LCOE} = \frac{\sum_{i=0}^{n} \frac{C_i}{(1+r)^i}}{\sum_{i=0}^{n} \frac{EY_0 \times (1-d)^i}{(1+r)^i}} \tag{1}$$

In eqn (1), C_i and EY_i are the costs and energy yields, respectively, for each year of operation, and these are summed over the

[a]University of Toledo, Wright Center for Photovoltaics Innovation and Commercialization, Department of Physics and Astronomy, 2801 W. Bancroft St., Toledo, OH, 43606, USA. E-mail: michael.heben@utoledo.edu

[b]South Dakota School of Mines and Technology, Department of Civil and Environmental Engineering, 501 E. St. Joseph St., Rapid City, SD, 57701, USA

† Electronic supplementary information (ESI) available. See https://doi.org/10.1039/d2se00029f

total time deployed in the field, n. C_i accounts for manufacturing and other initial installation costs (when $i = 0$) as well as ongoing maintenance and repair costs during the years of operation. The EY for each year depends on the incident irradiance, which varies with the time of the day, the day of the year, and location-specific aspects such as latitude, weather, and air pollution. Temperature variations are also important.[24,25] EY_i will diminish each year in accordance with the degradation rate, d. The net present value is evaluated by assuming a discount rate, r. In this work we used a discount rate of 6.5%, in agreement with others.[26] More details on the calculations are presented in the ESI.†

Several studies have examined the annual EY (AEY) of PK-containing tandem solar cells,[24,27–30] and a few other studies have evaluated the costs of fabrication.[31,32] Two studies estimated the fractional additional costs that would be required to obtain the higher efficiencies associated with a tandem,[33,34] while Li *et al.* performed a bottom-up cost analysis of PK/PK and PK/Si tandems and then estimated the LCOE by assuming average solar insolation and a PCE under a AM1.5G spectrum to determine the annual EY.[32] It was concluded that the LCOE of a PK tandem device could be lower than that of a PK SJ device because of the low-cost of adding a PK subcell. However, the PK cells were assumed to have already achieved a low degradation rate (1% per year) and a long deployment time (20 years).[32] To our knowledge, only one study has addressed the LCOE for a thin-film tandem of any kind, and this was done for CdTe/CIGS assuming an EY based on a clear-sky considerations.[31] In fact, there are no papers which consider the impacts of real-world EY on LCOE in tandems.

Currently, the most significant issue impeding commercialization of PK-based PV devices relates to stability issues.[35–41] While there have been significant advances in controlling degradation, PK-based devices have only demonstrated lifetimes on the order of a few thousand hours under illumination.[42–45] Successful PV technologies such as Si and CdTe require small degradation rates and long deployment times in the field so that investment of manufacturing and construction costs can produce many years of high EY. Large-scale investment and commercial adoption of PK-based tandems will be stimulated by the demonstration of substantially lower LCOE values than currently available options.

In this contribution, we investigate the impact of stability, SJ and tandem device efficiency, and manufacturing, installation, and operational costs on the LCOE. We use bottom-up cost models and real-world EY calculations to determine the LCOE values for SJ and PK-based tandems as a function of the degradation rate and presumed degradation mode for the PK subcell. We compare the LCOE for the individual SJ devices and investigate both 2T and 4T tandem deployments. As a representative case we focus on PK/CIGS tandems to leverage our previous real-world energy yield simulations[24] and technoeconomic analyses.[46] However, the conclusions are relevant to other tandems involving PK if the partner subcell has long-term stability (*e.g.*, Si, CIGS, CdTe).

Methods

Calculations were performed to assess AEY and manufacturing costs. Briefly, the AEYs for four different PV technologies (SJ PK, SJ CIGS, and 2T and 4T PK/CIGS tandems) were calculated by considering the real-world irradiance and temperature conditions in Phoenix, AZ. For these calculations, the hourly device performances were determined with the diode model, using the transfer matrix method (*via* measured refractive indices of all layers), and the hourly angle of incident, module temperature, spectral solar irradiance, and power distribution in the diffuse component of the light. Manufacturing steps and costs were used to determine the minimum sustainable price (MSP) of each PV technology. The MSP was determined as that cost at which the module price would yield the internal rate of return (IRR) equal to the weighted average cost of capital (WACC) for a manufacturer with 500 MW per year shipment, 7 year equipment depreciation, for a 25 year facility depreciation. The manufacturing steps and corresponding costs for each module is given in the ESI Tables S2 to S5.† For the cost component of the LCOE calculations, the MSP and installation costs were used as the initial cost for utility scale plant.

Results and discussion

The device architectures are shown in Fig. 1. The manufacturing costs of high performing SJ PK and CIGS devices with bandgaps of 1.55 and 1.16 eV, respectively, were determined following the work of others.[31,46] The bandgap combinations were chosen to optimize the real-world EY.[24] For the 2T device, we assumed the 1.16 eV CIGS device was fabricated first and that a 1.7 eV PK subcell was added to it. For the 4T device, the subcells were fabricated independently and combined with the encapsulant. The fabrication order and device structures were taken from champion device efforts.[8] The bottom cell fabrication consisted of deposition of a CIGS/CdS junction on a Mo back contact, topped with a ZnO buffer and an In_2O_3/SnO_2 (ITO) transparent top electrode. The top PK cell is fabricated in the p–i–n order with a solution-processed PK absorber material sandwiched between NiO and ZnO layers for hole and electron transport, respectively. ITO was used for both the back and front contacts. Fig. 1(e) shows that the manufacturing costs are dominated by the cost of materials, with the glass, junction box, encapsulant, edge seal, and ITO accounting for \$24 per m^2 in each case (ESI†). The absorber layer accounts for much of the difference between the devices, though the 4T device includes a second ITO layer and junction box. The depreciation was lower for the PK cell due to the lower equipment costs. The total manufacturing costs were \$50.91 per m^2 and \$34.02 per m^2 for the SJ CIGS and PK devices, and \$56.05 per m^2 and \$67.36 per m^2 for the 2T and 4T tandems, respectively.

We note that the PK material used as a top cell is different than the PK material used in the SJ cell and likely will include different material costs; however, this analysis shows that the PK material costs are \$1.05 out of the \$34.02 for the SJ cell, and most of it is due to the depreciation and maintenance of the deposition and processing equipment. As a result, to affect the

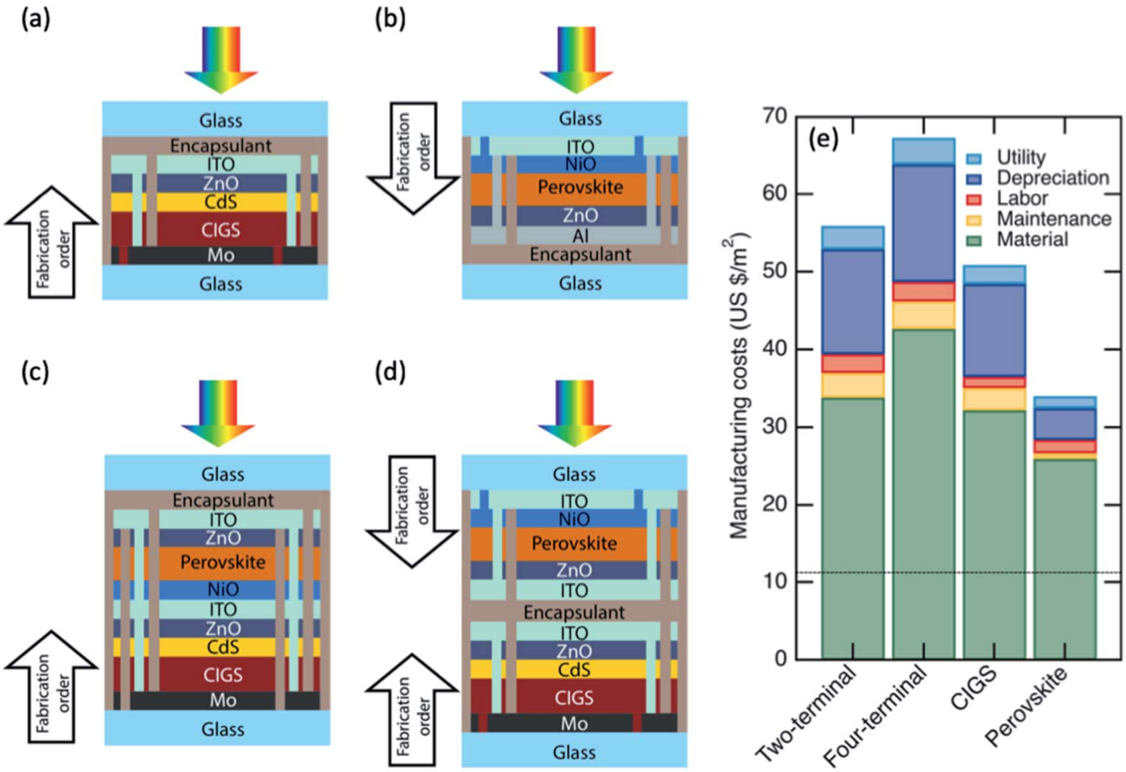

Fig. 1 Device structures and fabrication order for (a) 1.16 eV CIGS, (b) 1.55 eV perovskite, (c) two-terminal 1.16 eV CIGS/1.7 eV perovskite tandem, and (d) four-terminal 1.16 eV CIGS/1.7 eV perovskite tandem cells used to calculate the manufacturing costs. (e) Manufacturing cost breakdown for the modules are shown. The dashed line at 11.36 $ per m^2 corresponds cost for front and back glass.

overall cost structure of the SJ PK and tandem devices, the difference in cost between the 1.55 eV PK and 1.7 eV materials would need to be many-fold. Consequently, this cost difference between these two absorber materials was ignored.

We used the transfer matrix method and optical properties of each layer to calculate the external quantum efficiency,[47] and then determined the saturation current density at the thermodynamic limit. The irradiance data was used to determine the photogenerated current density. The current–voltage curves could then be simulated using the diode equation. Under AM1.5G irradiance, efficiencies for the SJ CIGS and PK devices were 24.9% and 24.8%, respectively, while the 2T and 4T tandems showed efficiencies of 33.0% and 33.7%. Dollar-per-watt values were determined to be $0.204 per W, $0.137 per W, $0.170 per W, and $0.200 per W, respectively. These values are in-line with other reports[31,32,46] and bench-mark well with the market after considering the off-setting effects of (i) calculated internal Shockley–Queisser limited performance that may be optimistic and (ii) bottom-up cost estimates that may over-estimate actual costs due to the savings that are available to manufacturers but not apparent to outsiders.[46]

By assuming mass production in the United States with a volume of 500 MW per year we were able to calculate a minimum sustainable price (MSP) for the sale of each type of module, following previous work.[31,46] Our results show, MSPs of 44.3, 75.8, 79.6 and 94.6 $ per m^2 for PK, CIGS, and 2T and 4T tandems, respectively. To check the sensitivity of our approach to manufacturing volume we reduced the volume by 50% (to 250 MW per year) and found increases the MSP by 19%, 33%, 36% and 34% for PK, CIGS, and 2T and 4T tandems, respectively. At a 50% higher manufacturing volume (750 MW per year) the MSPs were reduced by 6%, 11%, 12% and 11%, respectively. For the installed system we assumed a 100 MW utility-scale project with area of 0.525 km^2 located near Phoenix, AZ. The initial costs for the field consisted of the MSP for the modules and additional costs associated with the inverter(s), as well as area dependent costs associated with framing, wiring, land, and labor. After considering both the US Department of Energy's SunShot 2020 targets[48] and NREL's 2018 PV System cost benchmarks we adopted the more up-to-date values from the latter for the installation costs and costs of maintenance, repair, and annual operation.[49] While the former has higher inverter costs and lower operation and maintenance (O&M) costs, the values presented in the latter were determined to be more representative of today's marketplace [see ESI†]. In contrast to earlier studies,[31] we considered that 4T deployments will require additional inverters, wires, and labor during installation, as well as additional recurring O&M costs. Consequently, we investigated low, medium, and high incremental values for these of $0.04 per W and $2 per kW h, $0.08 per W and $4 per kW h, $0.16 per W and $6 per kW h, respectively. Details of the calculations, including cost of materials and other parameters, can be found in the ESI.†

To determine the initial EY for each module we followed our previous work with Phoenix AZ irradiance and meteorological data for each hour of the year with included average temperature variations.[24] To explicitly consider the impact of the stability of the PK cells on the LCOE as a function of degradation rate we followed industry norms[50,51] and defined the lifetime to be the time at which 85% of the initial output could still be generated, henceforth referred to as T85. Accordingly, the degradation rate, d, used in eqn (1) was expressed as shown in eqn (2).

$$d = 1 - 10^{\frac{\log(0.85)}{\mathrm{T85}}} \tag{2}$$

While the PK degradation rate varies, a 30 year T85 (degradation rate of 0.54% per year) is assumed for the CIGS SJ cells and subcells in both tandem architectures, a lifetime comparable to the best warranty that has been available in the industry.[52–54] With these degradation rates, we calculated the LCOE of the SJ and tandem devices.

Fig. 2(a) shows the LCOE of the SJ PK device as a function of T85, with the assumption that the deployment time equals the T85, while Fig. 2(b) shows that the LCOE for SJ CIGS device as a function of deployment time with the fixed degradation rate of 0.54%. As expected the LCOE becomes lower as the deployment time is extended. Fig. 2(a) also shows the tremendous advantages for PK in comparison to CIGS and, by extension, other technologies such as CdTe and Si. If stability issues can be addressed, the LCOE for a 30 year PK device would approach 4.6 cents per kW h, while the LCOE for the CIGS devices would be 5.6 cents per kW h. These results compare well with other reports for LCOEs for SJ PK[32,46] and CIGS devices,[31] which used different assumptions and inputs. Note that for comparison, the LCOE of Si is reported to be 5.1 cents per kW h with 30 year deployment.[49] We consider our work to be an improvement over past work due the use of state-of-the-art EY analysis as well as current best-guesses for device construction and process flow. Moreover, since our approach is comparative, it is internally self-consistent. A somewhat surprising result is that a PK device can achieve the same 30 year LCOE of a CIGS device with a T85, and, thus, deployment time, that is only $\frac{1}{2}$ as long.

For tandem devices, as for above, the PK subcell's lifetime was varied while the CIGS lifetime, T85, was fixed at 30 years, and we investigated how the T85 of the PK subcell affected the LCOE as a function of the deployment time of the tandem device. In the case of 4T devices, each subcell can operate independently so a separate degradation rate can be applied to each. Fig. 2(c) shows the LCOE of a 4T tandem as a function of the PK T85 and deployment time in the field. Note that the T85 of the PK subcell occurs when the performance degrades to 85% of the original value, so that subcell will continue to contribute to the overall EY of the tandem even after the T85 of the PK is reached if the devices is still deployed in the field. In addition, we assumed that the CIGS cell T85 and performance were not affected by degradation of the top PK cell. We also assumed low values ($0.04 per W and $2 per kW h) for the incremental balance of systems (BOS) installation and O&M costs, respectively (see ESI† for results with other assumptions). Interestingly, in comparing the data in Fig. 2(c) and (b) we see that adding a relatively short-lived PK cell (*e.g.*, T85 < 10 years) to a CIGS cell can produce lower LCOEs over a range of deployment times. As the PK stability improves, however, the LCOE advantage for pursuing a 4T tandem in comparison to a SJ PK device is reduced. While adding a PK subcell to a CIGS cell can lower the LCOE in comparison to the CIGS device by itself, a long-T85 SJ PK device would be preferred in comparison to the 4T option for the longer T85. The range over which the SJ PK device would be chosen over the 4T option depends on the incremental BOS and O&M costs (see ESI†).

In a 2T device the two subcells are in series and must operate with the same current. To examine the impact on the 2T performance we considered three different degradation modes for the PK cell: loss of current, loss of voltage, and loss of power. In these analyses the operating point for the 2T tandem and the AM1.5G efficiency was recalculated each year according to the change in the current–voltage characteristic for each mode of degradation. The initial EY was then reduced each year by the fraction of reduced AM1.5G efficiency. Once again, the CIGS degradation rate was held at 0.54% per year and the irradiance incident on the bottom cell was assumed to be unaffected by degradation of the PK cell. Clearly, this is a simplifying assumption since the degradation of the PK cell is expected to have a strong impact on the optical properties and transmission of light to the bottom cell. More detailed simulations would account for these changes, but are beyond the scope of the present effort. Although current loss and optical changes have been observed in unencapsulated PK device degradation studies,[35,55] a smooth decline in the output and a fairly constant change in the optical properties will be expected as the technology matures. Similarly, we can presume that stabilization of the maximum power point (MPP; or, roughly, fill factor) will become a critical factor for commercialization, and thus our approach can be considered to be a best-case scenario.

Fig. 2(d) shows the LCOE data for the PK subcell degrading at the MPP. For this case the voltage and current density at MPP were both degraded with $d^{1/2}$. Here we see clear benefits of adding a PK subcell. For example, adding a PK cell degrading at a 5 year T85 produces LCOEs near 5.4 cents per kW h when deployed in the field for 20 years. Such LCOEs are not produced by the SJ PK cell until a T85 of $\sim$17 years is reached. The purple (low LCOE) region in the figure is expanded significantly in comparison to the 4T data. Interestingly, at the longest T85 the LCOE for the 2T is only marginally better than the LCOE of the SJ PK device (4.5 *versus* 4.68 cents per kW h, respectively). The purple region in Fig. 2(d) at long T85 is somewhat smaller if the degradation is current-based and larger if the degradation is voltage-based (ESI†). Overall, the general trends are quite similar for each degradation mode, however the timescale of significant LCOE impact is more strongly effected for current degradation due to the current matching requirement for 2T tandems (see Fig. S5†).

Fig. 2(e) shows an "LCOE phase diagram" which delineates regions where a specific technology gives the lowest LCOE. The 4T option does not appear on this plot for even the low values of

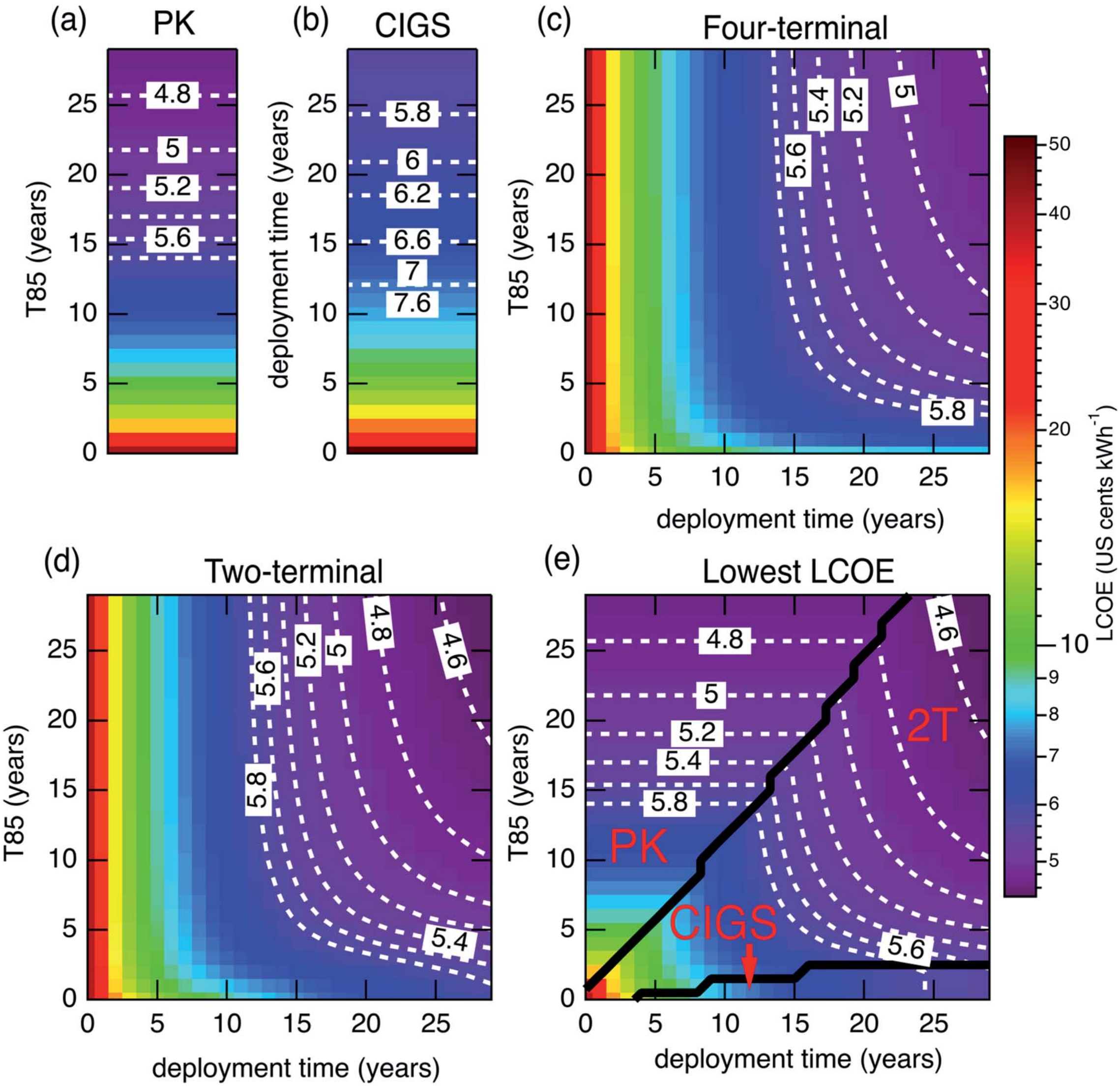

Fig. 2 LCOE in Phoenix, AZ of (a) PK single-junction device as a function of PK lifetime (T85) when the deployment time equals the lifetime; (b) CIGS single-junction device as a function of deployment time, and (c) four-terminal and (d) two-terminal tandems as a function of both the PK top cell T85 and deployment time. (e) The lowest LCOE approach as a function PK T85 and deployment time. White dotted lines are equi-LCOE contours, and black solid lines are region borders for the technologies with the lowest LCOEs. See text for more details.

the assumed incremental costs and for all PK degradation modes (see ESI†). The lack of the 4T option conflicts with the notion that added costs associated 4T operation can always be offset by higher efficiency and energy yield. The LCOE contours and the technology boundaries are also interesting to consider. When the PK T85 and deployment times are equal, the 2T tandem is preferred when MPP degradation is considered. Also, once again, a relatively short T85 PK device can significantly lower the LCOE for the field. For example, a PK subcell with a 10 year T85 (*i.e.*, one that is degrading at 1.6% per year) can produce an LCOE in a 2T field that is <5.2 cents per kW h for a deployment time of 20 years, and ~4.8 cents per kW h at 30 years. In this part of the plot, the 2T tandem is offering LCOEs similar to long-lived PK devices, but at much shorter PK T85.

While we have been focusing on PK/CIGS tandems, PK/Si devices are also of great interest. With estimated costs of manufacturing for the Si subcell at ~\$89.6 per m^2 by Li *et al.*[32] and ~\$68.3 per m^2 by Sofia *et al.*[56] as compare to \$34.02 per m^2 and \$50.91 per m^2 for PK and CIGS, respectively, one can assume that the LCOE for PK/Si tandems will be greater.[34] To explore the impact of the cost of the bottom cell on the LCOE, we varied the bottom cell cost while keeping its optical and electrical properties the same. The MSPs were then calculated for the 2T and 4T configurations, and the LCOE was determined for 30 year deployment in Phoenix, AZ. The results are shown in Fig. 3. If the manufacturing costs are below ~\$58 per m^2 the 2T module has the lowest LCOE for all values of PK T85 greater than 3 years. As the bottom cell cost increases the area of 2T preference shrinks and the SJ PK option become preferred at high PK T85, while for PK T85 shorter than 3 years the SJ form of the bottom cell is preferred regardless of bottom cell manufacturing cost. Interestingly, at high bottom cell cost and

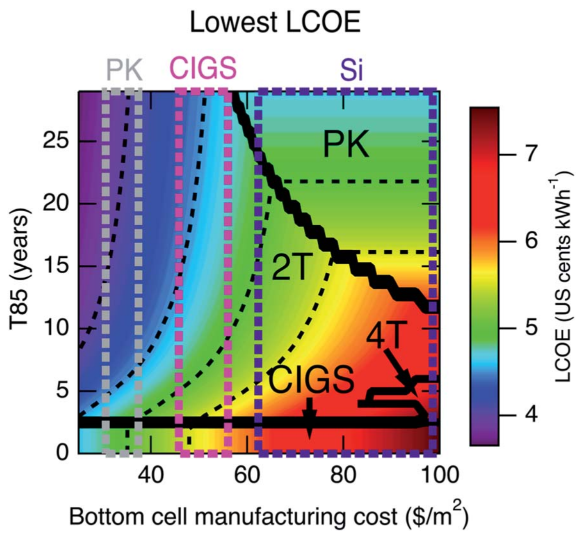

Fig. 3 LCOE phase diagram with differing top cell PK T85 and bottom cell manufacturing costs for devices in Phoenix, AZ. For the PK SJ devices, the LCOE values are calculated using a deployment time equal to the PK T85. For all other structures, the deployment time is 30 years. The 2T degradation mode and 4T incremental costs are the same as in Fig. 2 (MPP, and low values, respectively). The range of manufacturing cost between the dashed lines correspond to ±10% of the manufacturing cost estimates. For PK and CIGS bottom cells these are ±10% of \$34.2 per m^2 and \$50.9 per m^2, respectively. For Si bottom cell the range span from \$68.3 per m^2 minus 10% to \$89.6 per m^2 plus 10%.

low PK T85 there is a small region where the 4T option becomes preferred. Three price ranges are shown in Fig. 3, corresponding to ±10% of the manufacturing costs of PK, CIGS and Si as bottom cells. Clearly, low-cost, thin-film options in the 2T configuration will have the best chance of succeeding in the market.

It is worth noting that there has been a steady drop in the manufacturing costs of Si wafers.[57–59] This trend coincides with the improvements in the T85 and stability of PK solar cells. So far, most stable PK devices can operate within ~90% of their initial performances after a few thousands of hours of operation.[42–45] If one ignores the negative impact of stressing conditions (*e.g.* humidity, temperature)[35,36,39–41,60] and positive impact of performance recovery under no illumination,[61] a drop to 85% of initial state after 2000 hours of operation corresponds to approximately half a year of T85 lifetime considering the average sunshine hour count in Phoenix, AZ.[62] With further advancements, it is expected that the viability range of PK/Si tandems will extend to lower cost in the future. Note that this analysis considers the establishment of new manufacturing facilities and does not take into account capital investments that have already been made. Use of existing capital would change the economics in the short term, but would not greatly affect longer term scaling.

So far we have examined thermodynamically limited devices and ignored losses associated with cell-to-module integration. While record PCEs for SJ CIGS and PK devices are 94% and 102% (ref. 19) of the values calculated here, the highest reported efficiency for a 2T PK/CIGS device, 24.2%,[19] is only 73% of our thermodynamic value. The PK record is higher than our calculation because we chose materials based on a balance between cost and performance and did not apply an antireflection coating. Fig. 4 shows the LCOE data when these real-world aspects and cell-to-module integration issues are considered. Here we have assumed the SJ CIGS and PK modules can be manufactured at the modelled costs and perform at 97% of the iSQ limit. We additionally assume a 3 point efficiency loss due to cell-to-module integration for both SJ and tandem configurations. This reduction in efficiency is associated with the loss in area due to cell interconnection *via* laser scribing and edge delete processes, and is the best achieved to date as documented by NREL for First Solar's CdTe technology.[19,63] Thus, the total area efficiencies for the CIGS and PK modules were set to 21.1% and 21.2%, respectively. With this approach today's record 24.2% PK/CIGS device could have a PCE of 21.2% at the module level, and a 2T module operating at 97% of iSQ would have a total area efficiency of ~29%. As before, the SJ CIGS degradation rate d was set to 0.54% per year, the PK subcells were degraded at MPP, degradation of the PK cell was assumed to not impact the underlying device, and the EY the tandems was accumulated for 30 years regardless of the PK T85.

Fig. 4 shows that 2T modules made with today's record performance (*i.e.* module PCE of 21.2%) is not worth fabricating from an LCOE perspective. As the efficiency of the tandem improves the SJ PK and CIGS modules become less preferred, and at module efficiencies greater than ~27% tandems become strongly preferred for PK T85 greater than ~3 years. Overall, the results indicate that PCE loss due to cell-to-module integration shrinks the viability of the SJ devices. Clearly, both a high PCE

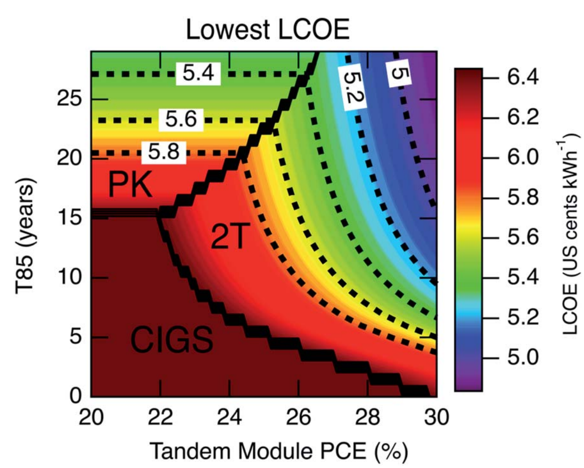

Fig. 4 LCOE phase diagram for tandems deployed in Phoenix, AZ as a function of PK T85 and module PCE. For the PK SJ devices, the LCOE values are calculated using a deployment time equal to the PK T85. For all other structures, the deployment time is 30 years. The single junction CIGS and PK module efficiencies were fixed at 21.1% and 21.2%, respectively. The 2T module efficiencies span from today's best research device efficiency to 97% of the iSQ limit, less 3 percentage points for cell-to-module integration (see text). Black dotted lines are equi-LCOE lines, and solid black lines indicate the borders of the lowest LCOE technologies.

and long T85 will be needed to access the lowest LCOEs values near 4.5 cents per kW h.

Throughout this study we have assumed that degradation in the PK device does not affect the output of the underlying CIGS device in the tandem configuration. Defining the lifetime to be when 85% of the initial output is still available suggests that degradation will proceed smoothly, over the course of years. Degradation studies of unencapsulated devices in the presence of high humidity, however, have shown that reactions with water cause the formation of PbI_2 with an associated bandgap widening from 1.7 eV to 2.3 eV. Depending on the device structure, other products could be $PbBr_2$ or PbO. More detailed modelling of the optical and electrical properties of the PK cell during these transformations would be required to determine the combined effects of more light entering the bottom CIGS subcell and the loss of electrical output from the top PK cell. While there is evidence for a degraded top PK cell being able to act as a transparent and conducting top device in a PK/Si tandem after PK degradation,[55] allowing some degree of operation of the Si cell to continue, the complexities of the changes in EY are beyond the scope of this study.

Conclusions

The conditions for viability of PK-based tandems were investigated. Costs associated with manufacturing and deployment of 2T and 4T PK/CIGS tandems were detailed and the LCOEs of tandem and SJ devices were determined as a function of PK T85 and degradation rate with real-world irradiance data for Phoenix, AZ. Because stability issues with PK-based devices generates uncertainty for large-scale deployment of both tandem and SJ devices, clear targets for the T85 of PK materials are needed. Our analysis indicates that PK T85 of 4 years are long enough to warrant the formation of a tandem device with lower LCOE than SJ CIGS and PK devices. We also determined that the manufacturing cost of the bottom cell has a significant impact on the economical viability of tandems, though this effect is larger at higher PK T85. We also showed that the PCE loss associated with cell-to-module integration further supports the case for low cost tandem construction as opposed to SJ modules. With tandem 2T PK/CIGS modules with PCEs above 27% and PK subcell T85 above 3 years, the tandems have lower LCOEs than SJ modules. Though such PCEs and stabilities are yet to be achieved, our findings point the way for future research.

Disclaimer

This report was prepared as an account of work sponsored by an agency of the United States Government. Neither the United States Government nor any agency thereof, nor any of its employees, makes any warranty, express or implied, or assumes any legal liability or responsibility for the accuracy, completeness, or usefulness of any information, apparatus, product, or process disclosed, or represents that its use would not infringe privately owned rights. Reference herein to any specific commercial product, process, or service by trade name, trademark, manufacturer, or otherwise does not necessarily constitute or imply its endorsement, recommendation, or favoring by the United States Government or any agency thereof. The views and opinions of authors expressed herein do not necessarily state or reflect those of the United States Government or any agency thereof.

The views and conclusions contained herein are those of the authors and should not be interpreted as necessarily representing the official policies or endorsements, either expressed or implied, of Air Force Research Laboratory or the U.S. Government.

Conflicts of interest

The authors declare no conflicts of interests for the work presented here.

Acknowledgements

This material is based upon work supported by the U.S. Department of Energy's Office of Energy Efficiency and Renewable Energy (EERE) under the Solar Energy Technologies Office Award Number DE-EE0008790 and by research sponsored by Air Force Research Laboratory under agreement number FA9453-18-2-0037. The U.S. Government is authorized to reproduce and distribute reprints for Governmental purposes notwithstanding any copyright notation thereon.

References

1 S. X. Tao, X. Cao and P. A. Bobbert, *Sci. Rep.*, 2017, **7**, 14386.
2 Y. Hou, E. Aydin, M. De Bastiani, C. Xiao, F. H. Isikgor, D.-J. Xue, B. Chen, H. Chen, B. Bahrami, A. H. Chowdhury, A. Johnston, S.-W. Baek, Z. Huang, M. Wei, Y. Dong, J. Troughton, R. Jalmood, A. J. Mirabelli, T. G. Allen, E. Van Kerschaver, M. I. Saidaminov, D. Baran, Q. Qiao, K. Zhu, S. DeWolf and E. H. Sargent, *Science*, 2020, **367**, 1135–1140.
3 J. Xu, C. C. Boyd, Z. J. Yu, A. F. Palmstrom, D. J. Witter, B. W. Larson, R. M. France, J. Werner, S. P. Harvey, E. J. Wolf, W. Weigand, S. Manzoor, M. F. A. M. Van Hest, J. J. Berry, J. M. Luther, Z. C. Holman and M. D. McGehee, *Science*, 2020, **367**, 1097–1104.
4 D. Kim, H. J. Jung, I. J. Park, B. W. Larson, S. P. Dunfield, C. Xiao, J. Kim, J. Tong, P. Boonmongkolras, S. G. Ji, F. Zhang, S. R. Pae, M. Kim, S. B. Kang, V. Dravid, J. J. Berry, J. Y. Kim, K. Zhu, D. H. Kim and B. Shin, *Science*, 2020, **368**, 155–160.
5 A. R. Uhl, A. Rajagopal, J. A. Clark, A. Murray, T. Feurer, S. Buecheler, A. K.-Y. Jen and H. W. Hillhouse, *Adv. Energy Mater.*, 2018, **8**, 1801254.
6 Y. H. Jang, J. M. Lee, J. W. Seo, I. Kim and D.-K. Lee, *J. Mater. Chem. A*, 2017, **5**, 19439–19446.
7 F. Fu, S. Pisoni, T. P. Weiss, T. Feurer, A. Wäckerlin, P. Fuchs, S. Nishiwaki, L. Zortea, A. N. Tiwari and S. Buecheler, *Adv. Sci.*, 2018, **5**, 1700675.

8 Q. Han, Y.-T. Hsieh, L. Meng, J.-L. Wu, P. Sun, E.-P. Yao, S.-Y. Chang, S.-H. Bae, T. Kato, V. Bermudez and Y. Yang, *Science*, 2018, **361**, 904–908.

9 M. Jost, T. Bertram, D. Koushik, J. Marquez, M. Verheijen, M. D. Heinemann, E. Köhnen, A. Al-Ashouri, S. Braunger, F. Lang, B. Rech, T. Unold, M. Creatore, I. Lauermann, C. A. Kaufmann, R. Schlatmann and S. Albrecht, *ACS Energy Lett.*, 2019, **4**, 583–590.

10 Y. Jiang, T. Feurer, R. Carron, G. T. Sevilla, T. Moser, S. Pisoni, R. Erni, M. D. Rossell, M. Ochoa, R. Hertwig, A. N. Tiwari and F. Fu, *ACS Nano*, 2020, **14**, 7502–7512.

11 D. H. Kim, C. P. Muzzillo, J. Tong, A. F. Palmstrom, B. W. Larson, C. Choi, S. P. Harvey, S. Glynn, J. B. Whitaker, F. Zhang, Z. Li, H. Lu, M. F. A. M. van Hest, J. J. Berry, L. M. Mansfield, Y. Huang, Y. Yan and K. Zhu, *Joule*, 2019, **3**, 1734–1745.

12 R. Lin, K. Xiao, Z. Qin, Q. Han, C. Zhang, M. Wei, M. I. Saidaminov, Y. Gao, J. Xu, M. Xiao, A. Li, J. Zhu, E. H. Sargent and H. Tan, *Nat. Energy*, 2019, **4**, 864–873.

13 J. Tong, Z. Song, D. H. Kim, X. Chen, C. Chen, A. F. Palmstrom, P. F. Ndione, M. O. Reese, S. P. Dunfield, O. G. Reid, J. Liu, F. Zhang, S. P. Harvey, Z. Li, S. T. Christensen, G. Teeter, D. Zhao, M. M. Al-jassim, M. F. A. M. Van Hest, M. C. Beard, S. E. Shaheen, J. J. Berry, Y. Yan and K. Zhu, *Science*, 2019, **364**, 475–479.

14 D. Zhao, C. Chen, C. Wang, M. M. Junda, Z. Song, C. R. Grice, Y. Yu, C. Li, B. Subedi, N. J. Podraza, X. Zhao, G. Fang, R.-G. Xiong, K. Zhu and Y. Yan, *Nat. Energy*, 2018, **3**, 1093–1100.

15 D. Zhao, Y. Yu, C. Wang, W. Liao, N. Shrestha, C. R. Grice, A. J. Cimaroli, L. Guan, R. J. Ellingson, K. Zhu, X. Zhao and R. Xiong, *Nat. Energy*, 2017, **2**, 1–7.

16 Z. Yu, Z. Yang, Z. Ni, Y. Shao, B. Chen, Y. Lin, H. Wei, Z. J. Yu, Z. Holman and J. Huang, *Nat. Energy*, 2020, **5**, 657–665.

17 Z. Yang, Z. Yu, H. Wei, X. Xiao, Z. Ni, B. Chen, Y. Deng, S. N. Habisreutinger, X. Chen, K. Wang, J. Zhao, P. N. Rudd, J. J. Berry, M. C. Beard and J. Huang, *Nat. Commun.*, 2019, **10**, 4498.

18 C. Chen, Z. Song, C. Xiao, R. A. Awni, C. Yao, N. Shrestha, C. Li, S. S. Bista, Y. Zhang, L. Chen, R. J. Ellingson, C.-S. Jiang, M. Al-Jassim, G. Fang and Y. Yan, *ACS Energy Lett.*, 2020, 2560–2568.

19 *NREL Best Research-Cell Efficiencies*, **https://www.nrel.gov/pv/cell-efficiency.html**.

20 T. Duong, H. Pham, T. C. Kho, P. Phang, K. C. Fong, D. Yan, Y. Yin, J. Peng, M. A. Mahmud, S. Gharibzadeh, B. A. Nejand, I. M. Hossain, M. R. Khan, N. Mozaffari, Y. L. Wu, H. Shen, J. Zheng, H. Mai, W. Liang, C. Samundsett, M. Stocks, K. McIntosh, G. G. Andersson, U. Lemmer, B. S. Richards, U. W. Paetzold, A. Ho-Ballie, Y. Liu, D. Macdonald, A. Blakers, J. Wong-Leung, T. White, K. Weber and K. Catchpole, *Adv. Energy Mater.*, 2020, **10**, 1–15.

21 M. Jošt, L. Kegelmann, L. Korte and S. Albrecht, *Adv. Energy Mater.*, 2020, **10**, 1904102.

22 N. R. E. Laboratory, *NREL System Advisory Model (SAM): Financial Model Documentation*, 2010.

23 S. Stephens, *Mater. Matters*, 2009, **4**, 99–102.

24 R. Hosseinian Ahangharnejhad, A. B. Phillips, K. Ghimire, P. Koirala, Z. Song, H. M. Barudi, A. Habte, M. Sengupta, R. J. Ellingson, Y. Yan, R. W. Collins, N. J. Podraza and M. J. Heben, *Sustainable Energy Fuels*, 2019, **3**, 1841–1851.

25 R. Hosseinian Ahangharnejhad, W. Becker, J. Jones, A. Anctil, Z. Song, A. Phillips, M. Heben and I. Celik, *Cell Rep. Phys. Sci.*, 2020, **1**, 100216.

26 D. Feldman, T. Lowder and P. Schwabe, *PV Project Finance in the United States*, 2016.

27 M. T. Hörantner and H. Snaith, *Energy Environ. Sci.*, 2017, **10**, 1983–1993.

28 M. T. Hörantner, T. Leijtens, M. E. Ziffer, G. E. Eperon, M. G. Christoforo, M. D. McGehee and H. J. Snaith, *ACS Energy Lett.*, 2017, **2**, 2506–2513.

29 J. Lehr, M. Langenhorst, R. Schmager, S. Kirner, U. Lemmer, B. S. Richards, C. Case, U. W. Paetzold, J. Lehr, M. Langenhorstb, R. Schmagerb, S. Kirnerc, U. Lemmera, B. S. Richards, C. Case and U. W. Paetzold, *Sustainable Energy Fuels*, 2018, **2**, 2754–2761.

30 M. Jošt, E. Köhnen, A. Morales Vilches, B. Lipovšek, K. Jäger, B. Macco, A. Al-Ashouri, J. Krc, L. Korte, B. Rech, R. Schlatmann, M. Topic, B. Stannowski and S. Albrecht, *Energy Environ. Sci.*, 2018, **11**, 3511–3523.

31 S. E. Sofia, J. P. Mailoa, D. N. Weiss, B. J. Stanbery, T. Buonassisi and I. M. Peters, *Nat. Energy*, 2018, **3**, 387–394.

32 Z. Li, Y. Zhao, X. Wang, Y. Sun, Z. Zhao, Y. Li, H. Zhou and Q. Chen, *Joule*, 2018, **2**, 1559–1572.

33 Z. J. Yu, J. V. Carpenter and Z. C. Holman, *Nat. Energy*, 2018, **3**, 747–753.

34 I. M. Peters, S. Sofia, J. Mailoa and T. Buonassisi, *RSC Adv.*, 2016, **6**, 66911–66923.

35 Z. Song, A. Abate, S. C. Watthage, G. K. Liyanage, A. B. Phillips, U. Steiner, M. Graetzel and M. J. Heben, *Adv. Energy Mater.*, 2016, **6**, 1600846.

36 P. Pistor, J. Borchert, W. Fra, R. Csuk and R. Scheer, *J. Phys. Chem. Lett.*, 2014, **5**, 3308–3312.

37 D. Bryant, N. Aristidou, S. Pont, I. Sanchez-molina, T. Chotchunangatchaval, S. Wheeler, R. Durrant and S. A. Haque, *Energy Environ. Sci.*, 2016, **9**, 1655–1660.

38 H. Yuan, E. Debroye, K. Janssen, H. Naiki, C. Steuwe, G. Lu, E. Orgiu, H. Uji-i, F. De Schryver, P. Samori, J. Hofkens and M. Roeffaers, *J. Phys. Chem. Lett.*, 2016, **7**, 561–566.

39 Z. Wang, Z. Shi, T. Li, Y. Chen and W. Huang, *Angew. Chem., Int. Ed.*, 2017, **56**, 1190–1212.

40 J. M. Frost, K. T. Butler, F. Brivio, C. H. Hendon, M. Van Schilfgaarde and A. Walsh, *Nano Lett.*, 2014, **14**, 2584–2590.

41 Z. Song, N. Shrestha, S. C. Watthage, G. K. Liyanage, Z. S. Almutawah, R. H. Ahangharnejhad, A. B. Phillips, R. J. Ellingson and M. J. Heben, *J. Phys. Chem. Lett.*, 2018, **9**, 6312–6320.

42 N. Arora, M. I. Dar, A. Hinderhofer, N. Pellet, F. Schreiber, S. M. Zakeeruddin and M. Grätzel, *Science*, 2017, **358**, 768–771.

43 G. Grancini, C. Roldán-Carmona, I. Zimmermann, E. Mosconi, X. Lee, D. Martineau, S. Narbey, F. Oswald, F. De Angelis, M. Graetzel and M. K. Nazeeruddin, *Nat. Commun.*, 2017, **8**, 15684.

44 J. A. Christians, P. Schulz, J. S. Tinkham, T. H. Schloemer, S. P. Harvey, B. J. T. de Villers, A. Sellinger, J. J. Berry and J. M. Luther, *Nat. Energy*, 2018, **3**, 68–74.
45 S. Ma, Y. Bai, H. Wang, H. Zai, J. Wu, L. Li, S. Xiang, N. Liu, L. Liu, C. Zhu, G. Liu, X. Niu, H. Chen, H. Zhou, Y. Li and Q. Chen, *Adv. Energy Mater.*, 2020, **10**, 1902472.
46 Z. Song, C. L. McElvany, A. B. Phillips, I. Celik, P. W. Krantz, S. C. Watthage, G. K. Liyanage, D. Apul and M. J. Heben, *Energy Environ. Sci.*, 2017, **10**, 1297–1305.
47 R. Hosseinian Ahangharnejhad, Z. Song, A. B. Phillips, S. C. Watthage, Z. S. Almutawah, D. R. SaPKota, P. Koirala, R. W. Collins, Y. Yan and M. J. Heben, *MRS Adv.*, 2018, **3**, 3111–3119.
48 R. Jones-Albertus, D. Feldman, R. Fu, K. Horowitz and M. Woodhouse, *Prog. Photovoltaics*, 2016, **24**, 1272–1283.
49 R. Fu, D. Feldman and R. Margolis, *U.S. Solar Photovoltaic System Cost Benchmark: Q1 2018*, 2018.
50 *First Solar Series 6™ 420-450 Watts Data Sheet*, 2020.
51 *Canadian Solar Limited Warranty Statement Photovoltaic HiDM Module Products*, 2020.
52 D. C. Jordan and S. R. Kurtz, *Photovoltaic Degradation Rates—An Analytical Review*, 2012.
53 D. C. Jordan and S. R. Kurtz, *Prog. Photovoltaics*, 2013, **21**, 12–29.
54 D. C. Jordan, S. R. Kurtz, K. VanSant and J. Newmiller, *Prog. Photovoltaics*, 2016, **24**, 978–989.
55 Z. Song, J. Werner, N. Shrestha, F. Sahli, S. De Wolf, B. Niesen, S. C. Watthage, A. B. Phillips, C. Ballif, R. J. Ellingson and M. J. Heben, *J. Phys. Chem. Lett.*, 2016, **7**, 5114–5120.
56 S. E. Sofia, H. Wang, A. Bruno, J. L. Cruz-Campa, T. Buonassisi and I. M. Peters, *Sustainable Energy Fuels*, 2020, **4**, 852–862.
57 M. Woodhouse, B. Smith, A. Ramdas and R. Margolis, *Crystalline Silicon Photovoltaic Module Manufacturing Costs and Sustainable Pricing: 1H 2018 Benchmark and Cost Reduction Road Map*, 2018.
58 Z. Xin-gang and W. Zhen, *Renewable Sustainable Energy Rev.*, 2019, **110**, 53–64.
59 Z. Liu, S. E. Sofia, H. S. Laine, M. Woodhouse, S. Wieghold, I. M. Peters and T. Buonassisi, *Energy Environ. Sci.*, 2020, **13**, 12–23.
60 C. C. Stoumpos, C. D. Malliakas and M. G. Kanatzidis, *Inorg. Chem.*, 2013, **52**, 9019–9038.
61 W. Nie, J. C. Blancon, A. J. Neukirch, K. Appavoo, H. Tsai, M. Chhowalla, M. A. Alam, M. Y. Sfeir, C. Katan, J. Even, S. Tretiak, J. J. Crochet, G. Gupta and A. D. Mohite, *Nat. Commun.*, 2016, **7**, 11574.
62 **https://nsrdb.nrel.gov/**.
63 *NREL Best Module Efficiencies*, **https://www.nrel.gov/pv/module-efficiency.html**.